

# Perspectives on QCD and EW physics from the Tevatron

---

**Robert Hirosky**<sup>\*†</sup>

*University of Virginia*

*E-mail:* [Hirosky@Virginia.Edu](mailto:Hirosky@Virginia.Edu)

This contribution to the 2015 meeting of the Deep Inelastic Scattering Workshop series summarizes recent physics results from the CDF and D0 Collaborations. Topics presented include: measurements using heavy flavor hadrons, top quark studies, parameters and properties of electroweak processes, boson+jet final states, and searches for new physics.

*The XXIII International Workshop on Deep Inelastic Scattering and Related Subjects*

*April 27 - May 1, 2015*

*Southern Methodist University*

*Dallas, Texas 75275*

---

<sup>\*</sup>Speaker.

<sup>†</sup>for the CDF and D0 Collaborations.

## 1. Introduction

The Run 2 physics program at the Fermilab Tevatron spanned the decade ending in September of 2011. Throughout Run 2 the CDF and D0 Experiments each collected  $\sim 10 \text{ fb}^{-1}$  of data from the world's highest energy  $p\bar{p}$  collisions at  $\sqrt{s} = 1.96 \text{ TeV}$ . Following the data collection, successful physics analysis programs have continued in both collaborations, with increasing focus on rare processes, precision measures, and measurements complimentary to those made by LHC experiments. This contribution to the 2015 meeting of the Deep Inelastic Scattering Workshop series summarizes recent Tevatron physics results. The reader is encouraged to refer to contributions by other speakers attending this workshop for more detailed reports on individual measurements.

## 2. Heavy flavor states

The programs of heavy flavor physics at CDF and D0 focus on studies of hadrons comprising one or more  $c$  or  $b$  flavored quarks. Heavy quark systems serve as valuable probes for a variety of fundamental physics studies, including studies of CP violation (CPV), effects of beyond the standard model (BSM) processes in rare decays and oscillation rates, tests of lattice gauge calculations, heavy quark effective theories, etc. This section summarizes recent measurements of decay properties and production asymmetries. The associated production of heavy flavored quarks in electroweak and QCD processes is discussed in the following sections.

### 2.1 Decay properties and symmetries

A recent study [1] by the D0 Collaboration reports a measurement of the  $B_s^0$  lifetime using the semileptonic decays  $B_s^0 \rightarrow D_s^- \mu^+ \nu X + \text{charge conjugate}$ . This measurement uses the full Tevatron Run 2 data sample comprising an integrated luminosity of  $10.4 \text{ fb}^{-1}$ . Using the flavor-specific final state, the charges of the decay products can be used to identify whether the meson was a  $B_s^0$  or  $\bar{B}_s^0$  at the time of decay. Due to flavor oscillations the measured lifetime is from a combination of heavy and light mass eigenstates in equal proportion at  $t = 0$ . The resulting lifetime is a superposition of two exponential distributions that can be modeled in  $\Gamma_s$ , the average decay width of the light and heavy states, and their difference  $\Delta\Gamma_s$ . The lifetime is measured using the pseudoproper decay length,  $\text{PPDL} = L_{xy} M / p_T(D_s^- \mu^+)$ , where  $L_{xy}$  is the transverse decay length of the  $B_s^0$  meson. Figure 1a shows the PPDL distribution for one of the data periods examined and includes signal and background projections. The measured flavor-specific lifetime is  $c\tau_{f_s}(B_s^0) = 443.3 \pm 2.9(\text{stat}) \pm 6.3(\text{sys}) \mu\text{m}$ , consistent with the current world average [2] and with smaller total uncertainty. The flavor-specific lifetime is an important parameter for extracting  $\Delta\Gamma_s$  in global fits and to constrain possible CP violation in the mixing and interference of  $B_s^0$  mesons as illustrated in Fig. 1b from the Heavy Flavor Averaging Group [3].

Both CDF and D0 report measurements of CP-violating asymmetries in the decay of  $D$  mesons. CDF measures the indirect CP-violating asymmetries  $A_\Gamma$  leading to differences in the effective lifetimes of charm and anticharm mesons in the decays  $D^0 \rightarrow K^+ K(\pi^+ \pi^-)$  [4] and D0 the direct CP-violating parameter  $A_{CP}(D^+ \rightarrow K^- \pi^+ \pi^+)$  [5] which measures the lifetime asymmetry in  $D^+$  and  $D^-$  mesons. The decay-time-dependent rate asymmetries for  $D^0$  meson decays provide sensitive probes for CP violating effects [6]. In the CDF analysis the  $D^0$  flavor is identified at production by

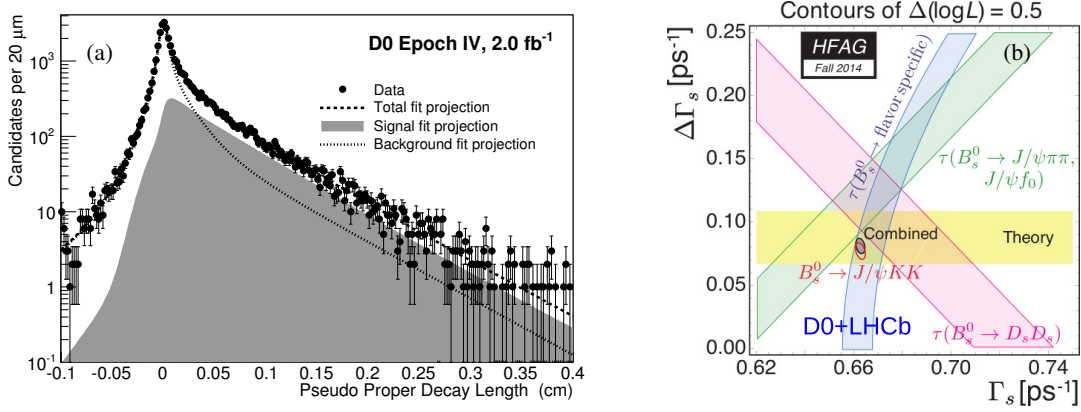


**Figure 1:** The (a) PDDL distribution of  $B_s^0$  candidates for one of the data periods in the D0  $B_s^0$  lifetime analysis. And (b) the global data fit to the  $\Gamma_s$  and  $\Delta\Gamma_s$  parameters by the Heavy Flavor Averaging Group [3].

selecting events from the strong decay process  $D^{*+} \rightarrow D^0\pi^+ + C.C.$  The decay-time-dependence of the asymmetry is shown in Fig. 2a for  $D^0 \rightarrow KK(\pi\pi)$  channels. These yield the asymmetry parameter  $A_\Gamma = [\hat{\tau}\bar{D}^0 - \hat{\tau}D^0]/[\hat{\tau}\bar{D}^0 + \hat{\tau}D^0] = (-0.12 \pm 0.12)\%$ . The results are consistent with the hypothesis of CP symmetry and can be used to improve global constraints on indirect CPV in charm-meson dynamics. The D0 measurement of charged  $D$  meson decays provides a high precision measurement of CPV parameters in Cabibbo favored decays, providing an experimental basis for the process which is assumed to be a charge symmetric process in various searches for CPV effects. The result, extracted from the multiplicities of  $D^{+/-}$  decays (Fig. 2c), is  $A_{CP}(D^+ \rightarrow K^- \pi^+ \pi^-) = [\Gamma(D^+) - \Gamma(D^-)]/[\Gamma(D^+) + \Gamma(D^-)] = [-0.16 \pm 0.15(stat) \pm 0.09(syst)]\%$  is consistent with the standard model (SM) prediction of CP conservation and improves the previous best measurement by a factor of 2.5 providing an important reference measurement for future studies of CP violation in charm and bottom hadron decays.

## 2.2 Production asymmetries

The production of  $b$  mesons at the Tevatron is dominated by gluon-gluon fusion with no forward-backward production asymmetry ( $A_{FB} = 0$ ), however contributions from  $qg$  and  $qq$  interactions, interference and EW processes can contribute to a non-zero  $A_{FB}$ . In  $p\bar{p}$  collisions we define a forward event to be one in which the  $b(\bar{b})$  quark follows the  $p(\bar{p})$  direction. D0 measures the production asymmetry for charged  $b$  mesons  $A_{FB}(B^\pm)$  using fully reconstructed decays  $B^\pm \rightarrow J/\psi(\rightarrow \mu^+\mu^-)K^\pm$ , where the sign of the  $B$  meson directly identifies the quark flavor. The asymmetry is measured in total and also differentially as a function of  $|\eta(B)|$  and  $p_T(B)$  (Fig. 3a)<sup>1</sup>. The total asymmetry of  $A_{FB}(B^\pm) = (-0.24 \pm 0.41 \pm 0.19)\%$  restricts the space for new physics causing anomalous F-B asymmetries in top and bottom decays, but is systematically lower than NLO predictions, implying that a more rigorous determination of the SM prediction is needed to interpret these results.

CDF presents two measures of production asymmetry in  $b$  quark pairs using  $b$ -tagged jets<sup>2</sup>.

<sup>1</sup>See contribution by B. Abbott to these proceedings.

<sup>2</sup>See contribution by J. Wilson to these proceedings.

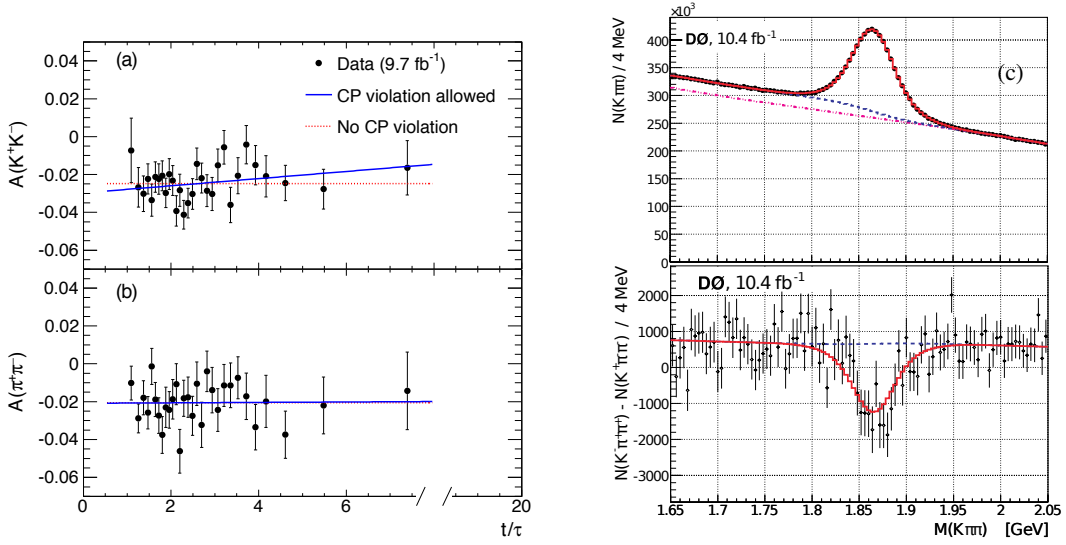


**Figure 2:** The (a,b) effective lifetime asymmetries as a function of decay time for  $D^0 \rightarrow K^+ K^- (\pi^+ \pi^-)$ . The (c) invariant mass distribution  $M(K\pi\pi)$  (top) and that for the difference in number of events  $N(D^+) - N(D^-)$  (bottom).

The analyses are separated by the dijet mass  $M_{bb}$  into low mass [8] and high mass [9] regions. The low mass analysis considers  $M_{bb} < 300$  GeV and is in good agreement with SM predictions (Fig. 3b). The high mass analysis (Fig. 3c) is consistent with zero and the SM. This result reduces the parameter space to produce  $t\bar{t}$  asymmetries and is used to exclude a range of axigluon models with mass  $\sim 200$  GeV.

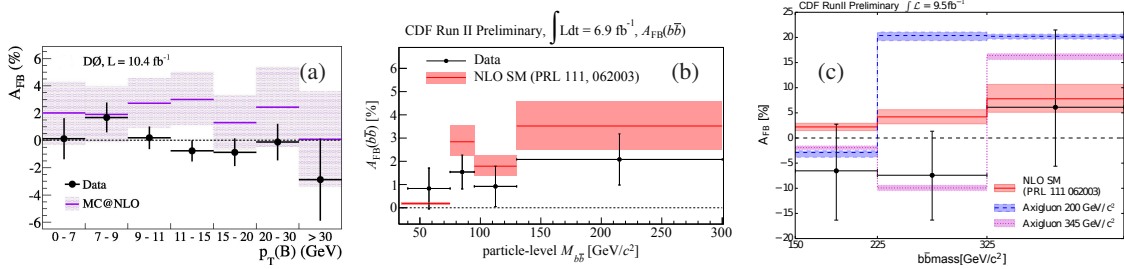


**Figure 3:** The (a) D0 comparison of  $A_{FB}(B^\pm)$  and  $A_{FB}^{SM}(B^\pm)$  in bins of  $p_T(B^\pm)$ . CDF measured  $A_{FB}$  (b) as a function of particle-level  $M(b\bar{b})$  for the low  $b\bar{b}$  mass analysis and (c) maximum a posteriori points for the signal asymmetry in each mass bin of the high mass  $b\bar{b}$  analysis.

D0 also examines the forward-backward asymmetries in production of  $\Lambda_b^0$  and  $\bar{\Lambda}_b^0$  [10]. The measurement is sensitive to hadronization effects, such as the “string drag” model [11] illustrated in Fig. 4a. The result shown in Fig. 4b is in general agreement with expectations from the heavy quark drag model. D0 also presents a new measure of  $A_{FB}$  in the production of  $\Lambda^0$  and  $\bar{\Lambda}^0$  baryons [12]. This measure of  $A_{FB}$  is consistent with a strong connection to the quark flavor of the incoming hadron. The  $\bar{\Lambda}^0/\Lambda^0$  ratio is shown to be approximately a universal function of the proton “rapidity loss”  $y_p - y_\Lambda$  with little dependence on  $\sqrt{s}$ , target type, or kinematic factors, see Fig. 4c.

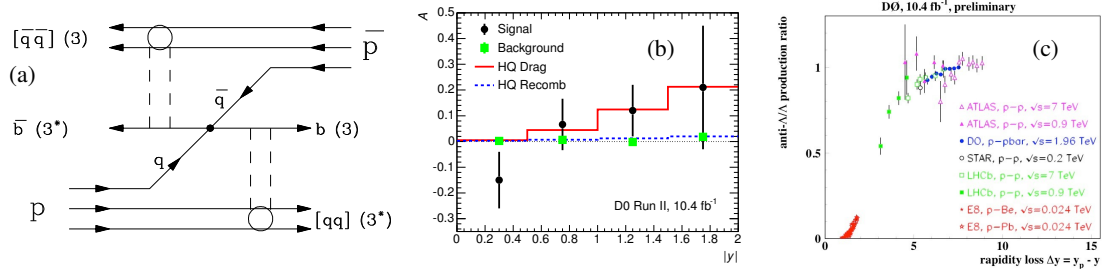


**Figure 4:** Illustration (a) of string drag effect in  $\Lambda_b$  production. The (b) measured forward-backward asymmetry  $A$  versus rapidity  $|y|$  compared to predictions of the Heavy Quark Recombination model [13] and a simulated effect of the longitudinal momentum shift due to beam drag [11]. The (c)  $\bar{\Lambda}^0/\Lambda^0$  ratio as a function of the rapidity loss in multiple experiments.

### 3. Top quark

Following the discovery of the top quark by CDF and D0 in 1995, both experiments have pursued a rich program of study into top quark properties and production characteristics in the Run 2 data. The unique nature of the  $p\bar{p}$  initial state at the Tevatron allows for a variety of measurements that offer more precision or are complementary to those performed at the LHC. The final combination of CDF and D0 measurements [14] of cross sections for single top quark production is presented using an integrated luminosity of up to  $9.7 \text{ fb}^{-1}$ . Both t-channel and s+t-channel cross sections are measured yielding  $\sigma_t = 2.25^{+0.29}_{-0.31} \text{ pb}$  and  $\sigma_{s+t} = 3.30^{+0.52}_{-0.40} \text{ pb}$ . The resulting 2D posterior probability distribution as a function of  $\sigma_t$  and  $\sigma_s$  is presented in Fig. 5(a) along with predictions based on SM calculations [16, 17] and various non-SM scenarios [18, 19, 20]. The SM single-top-quark production cross section is approximately proportional to the square of the CKM matrix element  $V_{tb}$ . Assuming that top quarks decay exclusively to  $Wb$  final states, the combined data is used to extract the best fit value  $|V_{tb}| = 1.02^{+0.06}_{-0.05}$  as illustrated in Fig. 5b. The limit  $|V_{tb}| > 0.92$  is set at the 95% C.L. by restricting the prior to the SM region [0,1].

Measures of the top quark mass  $m_t$  have achieved unprecedented precision with increased data samples and refinements in measurement techniques. The D0 measure of  $m_t$  in  $9.7 \text{ fb}^{-1}$  of Run 2 integrated luminosity presented at DIS2015 uses a matrix element technique in  $t\bar{t}$  candidate events in the lepton+jets final states. A detailed description of this analysis is given in Ref. [21]. The calibration  $k_{\text{JES}}$  of the overall jet energy scale (JES) is performed in situ taking into account all kinematic information in a given event and applying the constraint from the reconstructed invariant mass of the  $W \rightarrow q\bar{q}'$  decays (Fig. 6a). Figure 6b shows the invariant mass of the dijet system matched to one of the  $W$  bosons in the  $e$ +jets final state. The result  $m_t = 174.98 \pm 0.58(\text{stat} + \text{JES}) \pm (\text{syst}) \text{ GeV}$  with an uncertainty of 0.43% constitutes the most precise single measurement of  $m_t$  at the time of this workshop with a total systematic smaller than any other single experiment.

Also presented at DIS2015 for the first time is a new D0 measure of the top quark mass in the dilepton decay channel using an optimized neutrino weighting method [22]. First results are presented in H. Liu's contribution to this conference.

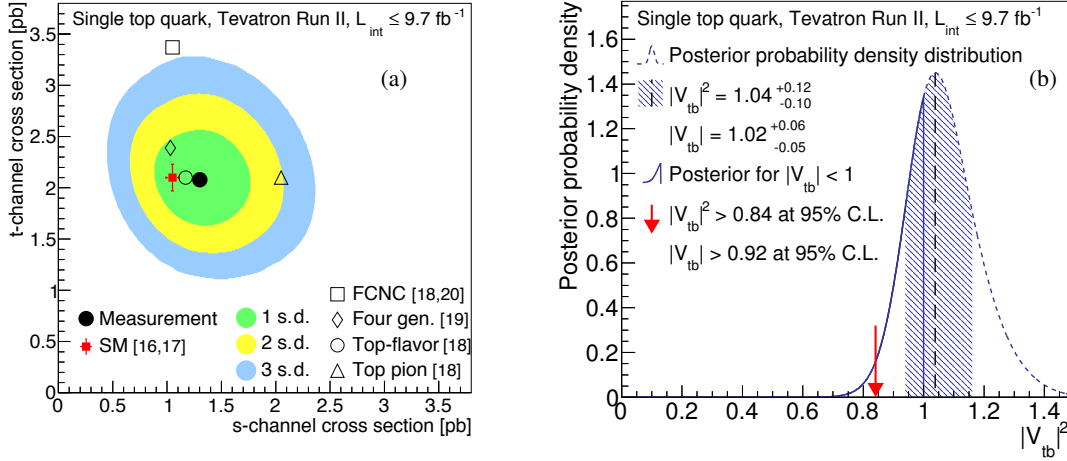


**Figure 5:** The (a) two-dimensional posterior probability as a function of  $\sigma_t$  and  $\sigma_s$  for the combined CDF and D0 data compared with the NLO+NNLL theoretical prediction of the SM [15]. Predictions from several BSM predictions are also shown. The (b) posterior probability distribution versus  $|V_{tb}|^2$  for the combination of the CDF and D0 data.

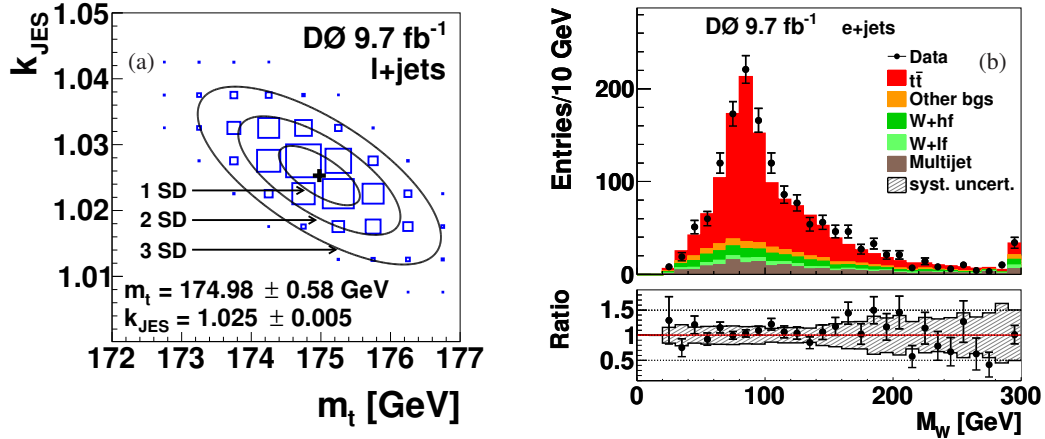


**Figure 6:** The (a) 2D likelihood for the D0 measurement of  $m_t$  and the jet energy scale calibration factor  $k_{JES}$  in lepton+jets final states. The (b) invariant mass of the dijet system matched to the hadronically decaying  $W$  boson in the  $e$ +jets final state.

## 4. Electroweak physics

Large data samples, low backgrounds, and precise calibration techniques facilitate a wide range of electroweak studies by the Tevatron experiments.

### 4.1 $W$ and $Z$ production and decay

A recent measurement [23] of the electron charge asymmetry in  $p\bar{p} \rightarrow W + X \rightarrow e\nu + X$  events by D0 is presented as a function of the electron pseudorapidity in a variety of kinematic bins based on the electron transverse energy and missing transverse energy in the event. The measured asymmetry is compared with next-to-leading-order predictions in perturbative quantum chromodynam-

ics (pQCD) and a variety of PDF models, as partially summarized in Fig. 7. The D0 measurement is the most precise lepton charge asymmetry measurement to date and these data provide additional and precise information for determining the parton distribution functions of the proton.

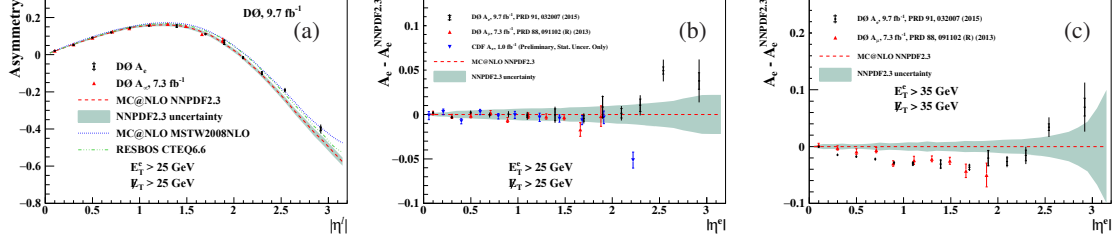


**Figure 7:** The lepton charge asymmetry distribution (CP invariance assumed) with kinematic cuts as shown. Comparison (a) of the measured asymmetry with predictions and differences (b,c) between data and MC predictions based on the central value from MC@NLO [24] with the NNPDF2.3 PDF set [25].

A new determination [26] of the effective weak mixing angle  $\sin^2\theta_{eff}$  at D0 is presented from measurements of the distribution of the forward-backward charge asymmetry  $A_{FB}$  in the process  $p\bar{p} \rightarrow Z/\gamma^* \rightarrow e^+e^-$ . This measure significantly extends the electron acceptance from a previous report [27] and introduces a new electron energy calibration method, reducing the primary systematic uncertainty. The final result from  $9.7 \text{ fb}^{-1}$  of integrated luminosity,  $\sin^2\theta_{eff} = 0.23146 \pm 0.00047$ , is the most precise measurement from light quark interactions and is close in precision to that obtained from  $e^+e^-$  colliders (Fig. 8a).

The variable  $\phi_\eta^*$  [28] provides unprecedented precision to study the  $p_T^{\ell\ell}$  distribution in decays of  $Z/\gamma^*$  bosons in  $ee$  and  $\mu\mu$  final states. D0 presents measurements of the normalized  $\phi_\eta^*$  in Drell-Yan muon pairs in bins of dimuon rapidity. The measurement is extended to “off-peak” samples of dimuon events and considers ranges of  $M_{\ell\ell}$  between 30 and 500 GeV. Figure 8b shows the ratio of the  $(1/\sigma)(d\sigma/d\phi_\eta^*)$  distribution for  $M_{\ell\ell} \sim m_Z$  in the rapidity regions ( $|y| < 1$ )/( $1 < |y| < 2$ ) compared with the prediction from NNLL+NLO calculations [29]. Theoretical uncertainties largely cancel in this ratio and the predictions are found to be consistent with the data. The ratio of the  $\phi_\eta^*$  distributions in data to RESBOS [30] (NNLL+NLO) calculations for  $30 < M_{\ell\ell} < 60$  is shown in Fig. 8c(d). The disagreement at large  $\phi_\eta^*$  for RESBOS may arise from the absence of the NNLO correction factor for the photon exchange diagram.

## 4.2 Dibosons

A measurement of the associated diboson production  $WW$  and  $ZZ$  by CDF considers the final state consistent with semileptonic  $W$  decay plus heavy flavor quarks [31]. For the first time at a hadron collider, this result uses the different heavy flavor decay patterns of the  $W$  and  $Z$  bosons (i.e.  $W^+ \rightarrow c\bar{s}; Z \rightarrow b\bar{b}, c\bar{c}$ ) and properties of the secondary-decay vertex to independently measure the  $WW$  and  $WZ$  production cross sections in a hadronic final state. Figure 9a shows the dijet invariant mass  $M_{inv}(\text{jet}_1, \text{jet}_2)$  for events with two heavy-flavor-tagged jets, which is sensitive to  $WZ$  production. The production cross sections for  $WW/WZ$  in the HF-enriched final state are determined using a Bayesian statistical analysis considering data, signal, and background estimates together with all rate and/or shape systematic uncertainties treated as nuisance parameters. Figure 9b shows

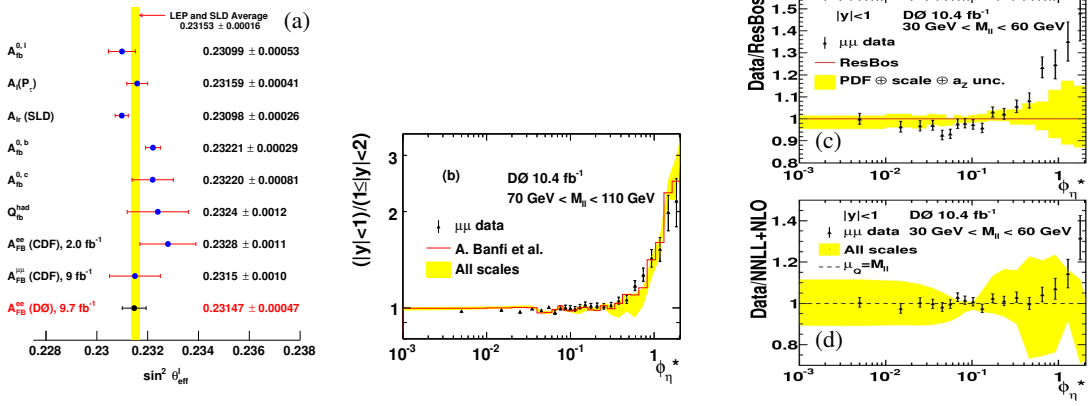


**Figure 8:** Comparison (a) of measurements of  $\sin^2 \theta_{eff}$  with the recent D0 measurement. Ratio (b) of the  $(1/\sigma)(d\sigma/d\phi_{\eta^*})$  distribution in central and forward rapidity regions for  $Z/\gamma^*$  compared with the NNLL+NLO calculation. Ratio of the  $(1/\sigma)(d\sigma/d\phi_{\eta^*})$  distribution in the central rapidity region to RES-BOS (c) and NNLL+NLO (d) calculations in dimuon events with  $30 < M_{\ell\ell} < 60 \text{ GeV}$ .

the measured Bayesian posterior distribution for  $\sigma_{WW}$  and  $\sigma_{WZ}$  where each cross section is allowed to float independently. The two-dimensional posterior distribution is projected onto each axis and used to obtain the individual cross sections  $\sigma_{WW} = 9.4 \pm 4.2 \text{ pb}$  and  $\sigma_{WZ} = 3.7_{-2.2}^{+2.5} \text{ pb}$ , measuring for the first time the two processes independently in a hadronic final state.

A second diboson measurement by CDF examines the differential production cross section for  $WW$  as a function of associated jet multiplicity and jet  $p_T$  [32], for case of associated production with one jet. The differential  $WW$  cross section is extracted comparing neural net output shapes in data to signal and background in each signal region using a binned maximum likelihood method. To account for effects of bin to bin migration of events due to jet reconstruction, scale, and resolution effects, the result is unfolded to the hadronic level using a Bayesian method. The measured values are compared with predictions from ALPGEN [33], MC@NLO, and scale factors for the differential and inclusive cross sections. The results are consistently high but within one standard deviation, except for the two or more jet bin, which is within two standard deviations. The measured inclusive cross section of  $14.0 \pm 0.6(stat)_{-1.3}^{+1.6}(syst)$  is consistent with the Standard Model prediction and is the most precise measurement of the  $WW$  cross section at a  $p\bar{p}$  collider.

### 4.3 $V + \text{heavy flavor}$

Both CDF and D0 have explored a wide and increasingly rare variety of processes leading to vector boson ( $V = W, Z$ ) plus heavy flavor (HF) final states. For example, the standard model production of  $W/Z + \Upsilon$  may occur through parton-level processes producing  $W/Z + b\bar{b}$  with the  $b\bar{b}$  pair then forming a bound state. Cross sections at the Tevatron for  $W(Z) + \Upsilon$  are calculated to be only 43(34) fb [34]. However charged Higgs bosons or further light neutral scalars may decay into  $W(Z) + \Upsilon$  states, respectively, thus observation of  $W(Z) + \Upsilon$  production above the predicted SM rate may indicate the presence of physics not described by the SM. CDF performed a new search [35] for  $W(Z) + \Upsilon$  production using 9.4  $\text{fb}^{-1}$  of Run 2 data. A candidate event is displayed in Fig. 10a. In the analysis no significant excess of events is observed with respect to standard

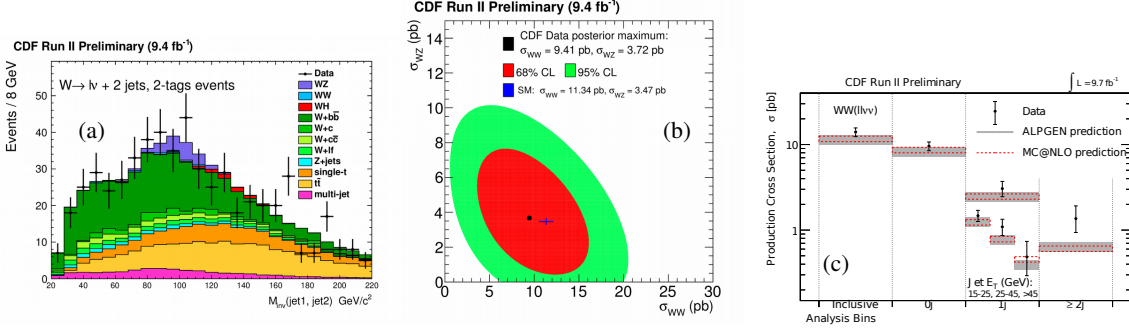


**Figure 9:** The (a)  $M_{inv}(jet_1, jet_2)$  distribution for candidate events with 2  $b$ -tagged jets in the CDF WW/WZ analysis. Bayesian posterior (b) shown in the plane  $\sigma_{WW}$  versus  $\sigma_{WZ}$ . The filled areas represent the smallest intervals enclosing 68% and 95% of the posterior integrals, respectively. CDF measurements (c) of inclusive and differential cross section measurements and predictions for WW(+jets).

model background predictions, therefore 95% C.L. upper limits are set at  $\sigma(p\bar{p} \rightarrow W\Upsilon) < 5.6$  pb and  $\sigma(p\bar{p} \rightarrow Z\Upsilon) < 21$  pb. These are the most stringent bounds on  $W/Z + \Upsilon$  processes to date.

The first measurement of the differential cross section as a function of  $p_T^{jet}$  for the associated production  $W + b$ -jet and  $W + c$ -jet [36] is presented by D0 using events where the  $W$  boson decays as  $W \rightarrow \mu\nu$ . These are the first measurements of  $W + b/c$  cross sections that are sensitive to the gluon splitting processes. Sensitivity to gluon splitting is preserved removing any requirement on a soft lepton within jets used in the analysis. The measured  $W + b$ -jet cross section shown in Fig. 10b is systematically higher than predictions of NLO perturbative QCD and is suggestive of missing higher order corrections. The measured  $W + c$ -jet cross section (Fig. 10d) agrees with the NLO pQCD prediction at low  $p_T^{c-jet}$ , but the disagreement towards high  $p_T^{c-jet}$  may indicate missing higher order corrections, an underestimated contribution from gluon splitting and/or possible enhancement in the strange quark PDF.

Studies of  $Z$  boson production in association with a bottom and an antibottom quark provide important tests of the predictions of perturbative quantum chromodynamics. A good description of this process is essential since it forms a major background for a variety of physics processes. D0 presents the ratio of  $Z + 2b$  jets to  $Z + 2$  jets inclusive production cross sections [37]. In the ratio many systematic uncertainties are canceled and the relative rate to  $Z + 2$  jets may be more precisely compared to SM predictions. Figure 10c shows the distribution of the D0  $b$ -jet discriminant  $D_{MJJL}$  for the highest- $p_T$  jet in the  $Z$ +heavy flavor analysis for data, light and heavy jet flavor templates using decays  $Z \rightarrow ee(\mu\mu)$ . The ratio of the integrated cross sections  $\sigma(p\bar{p} \rightarrow Z + 2bjet)/\sigma(p\bar{p} \rightarrow Z + 2jet)$  is measured in the restricted phase space  $p_T^\ell > 15$  GeV  $|\eta^\ell| < 2.0$  and two jets satisfying  $p_T^{jet} > 20$  GeV and  $|\eta^{jet}| < 2.5$  yielding the ratio  $0.0236 \pm 0.0032(\text{stat}) \pm 0.0035(\text{syst})$  in agreement with theoretical predictions within uncertainties.

## 5. Searches for clues of new physics

The unique  $p\bar{p}$  initial state along with low trigger thresholds and reduced background for a variety of signals provide windows of sensitivity complimentary to those at the LHC to search for new physics processes. Several of these searches are summarized in this section.

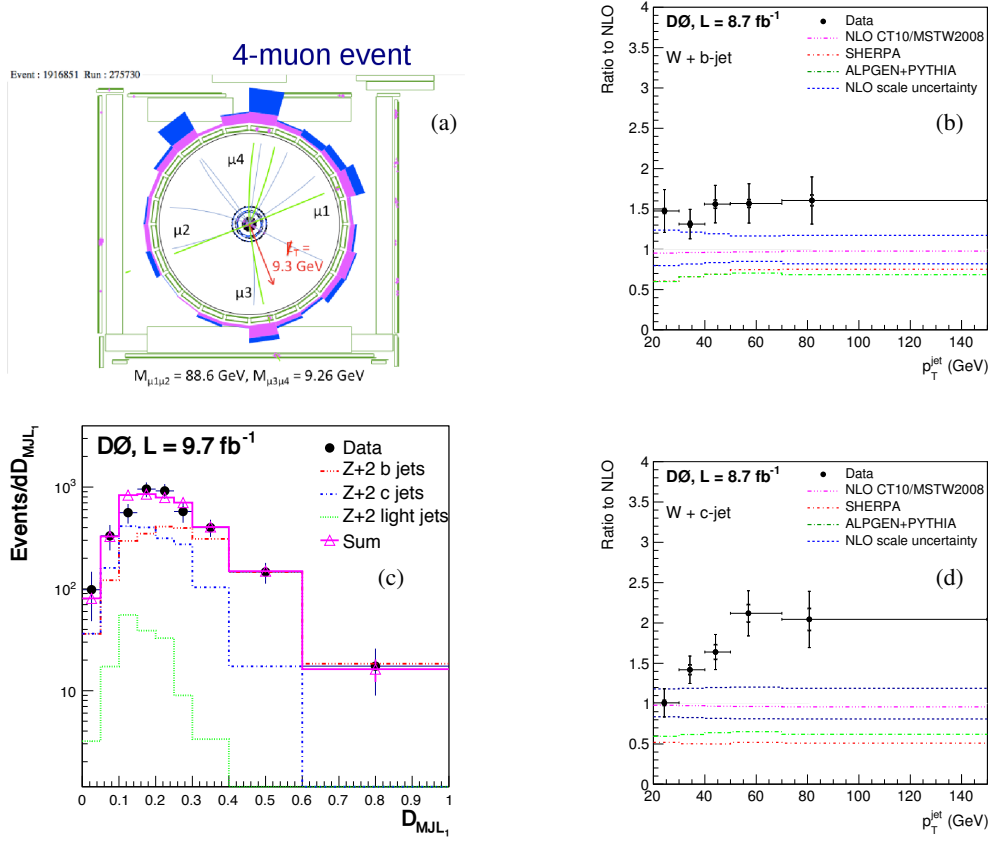


**Figure 10:** A  $Z + \Upsilon$  event candidate (a) from CDF. Ratio of the D0 measurement of the (b)  $W + b$ -jet and (d)  $W + c$ -jet production cross sections to theoretical predictions. Distribution (c) of the D0  $b$ -jet discriminant  $D_{MJL}$  [37] for the highest- $p_T$  jet in the  $Z$ +heavy flavor analysis for data, light and heavy jet flavor templates.

CDF presents a search for charged massive resonances [38] decaying to a  $tb$  quark pair in events where the top quark decays to a  $Wb$  pair and the  $W$  boson decays to a charged lepton and a neutrino. The topology of these decays is similar to that in  $t$ -channel single top production. This search is sensitive to any narrow resonant state decaying to  $tb$  and is used to test a benchmark model of  $W'$  bosons of unknown mass with universal weak-coupling strength to SM fermions and considers the case of either allowed or forbidden leptonic decay modes ( $W' \rightarrow \ell\nu$ ) for the  $W'$ . The only effect of the latter is to increase the branching fraction  $\mathcal{B}(W' \rightarrow tb)$ . Background rejection is accomplished using an artificial neural network to separate the dominant QCD multijet background from signal and other backgrounds, followed by two additional neural networks to classify events according to expectation from  $V$ +jets and  $t\bar{t}$  backgrounds and which are used to define the signal discriminant  $NN_{sig}$ . The expected and observed final discriminant distribution for one of the signal regions is shown in Fig. 11a. The data are consistent with the background-only expectations and used to set upper limits on the production cross-section times branching ratio at the 95% Bayesian credibility. For a specific benchmark model (left-right-symmetric SM extension)  $W'$  bosons with masses lower than 860(880) GeV are excluded in cases there the  $W'$  leptonic-decay is allowed (for-

bidden). This search yields the most constraining limits to date on narrow  $tb$ -resonance production for masses smaller than about 600 GeV (see Fig. 11b). Another analysis by CDF searches for evidence of Dirac magnetic monopoles produced via Drell-Yan processes [39]. This analysis uses a dedicated trigger for the expected highly ionizing signature of monopole interactions. A custom detector simulation is employed as is a specialized offline reconstruction algorithm for tracks that do not curve perpendicularly to the CDF central magnetic field. Figure 11c shows the comparison between CDF and ATLAS limits for the Drell-Yan production model. Plotted is the ratio of the 95% CL limit to prediction as a function of the mass of the monopole for the two experiments. In the CDF analysis a 95% C.L. cross section limit is set for masses in the range 300–600 GeV of approximately 6 fb and 11 fb for the range 100–800 GeV. For a Drell-Yan production model, monopoles are excluded for mass less than 476 GeV and the CDF analysis provides the most sensitive limits for masses less than 300 GeV.

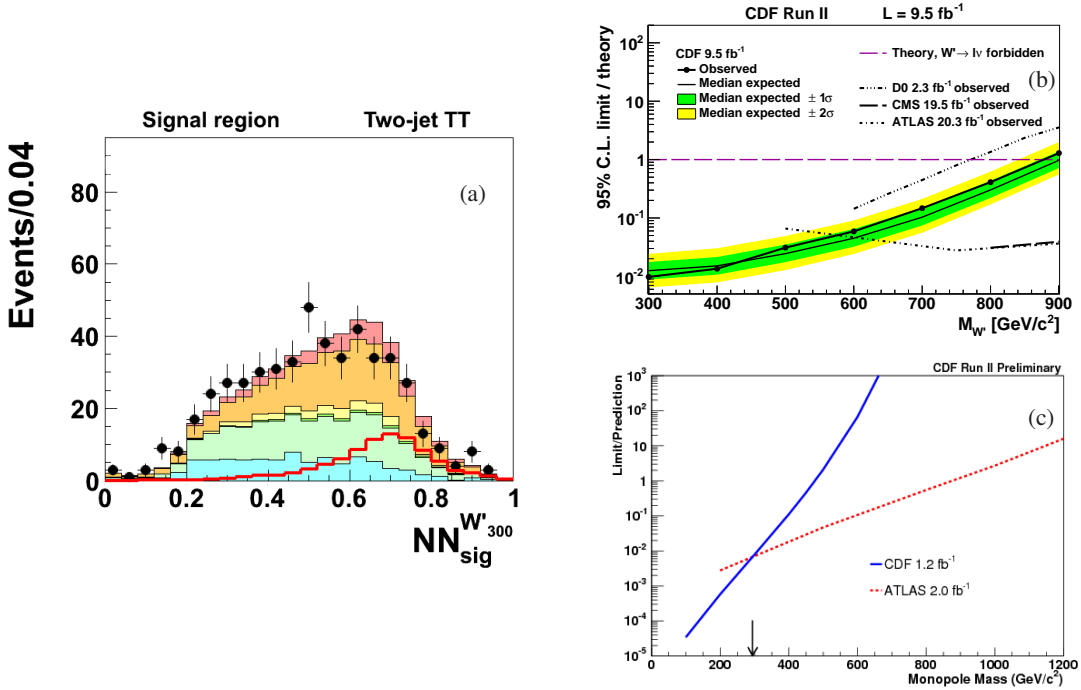


**Figure 11:** Expected and observed final discriminant distribution (a) for one of the signal regions the CDF  $W'$  searches and the (b) observed and expected limits on the cross section times branching fraction for the benchmark  $W'$  boson model with forbidden decay mode  $W' \rightarrow \ell\nu$ . Comparison (c) between CDF and ATLAS limits for the Drell-Yan production model of Dirac monopoles.

Finally, a combined Tevatron analysis sets constraints on models of the Higgs boson with exotic spin and parity [40]. CDF and D0 previously reported evidence [41] for an excess of events consistent with a Higgs boson signal, largely driven by channels sensitive to the decay of the Higgs boson to bottom quarks ( $H \rightarrow b\bar{b}$ ). Results of the study presented in Ref. [42] describe the effects on final state kinematic distributions for the production of an exotic resonance  $X \rightarrow b\bar{b}$  with pseudoscalar ( $J_P = 0^-$ ) or gravitonlike ( $J_P = 2^+$ ) spin and parity. The particle decaying fermionically for which the Tevatron found evidence might not be the same as the Higgs particle discovered through its bosonic decays at the LHC. Tests of the spin and parity with Tevatron data

therefore provide unique information on the identity and properties of the new particle or particles. Employing re-optimized analyses in  $W(Z) + H, H \rightarrow b\bar{b}$  channels, CDF and D0 report combined studies of the  $J^P$  assignments of the state  $X \rightarrow b\bar{b}$ , with  $m_X = 125$  GeV. Figure 12a shows the distribution  $\log_{10}(s/b)$  for the combined CDF and D0 data computed from all channels contributing to the  $J_P = 0^-$  search. The backgrounds are fit to the data, with systematic uncertainties allowed to vary within their a priori constraints. The exotic signal is normalized to the SM cross section times branching ratio for  $H \rightarrow b\bar{b}$  multiplied by a scaling factor  $\mu_{\text{exotic}} = 1$  in this figure. The chosen value of  $\mu_{\text{exotic}}$  is arbitrary and the sensitivity of the analysis is reduced for smaller values. Bayesian upper limits are quoted and the modified frequentist (CLs) method [43] is used to perform hypothesis tests. Distributions of the LLR= $-\ln(p(\text{data}|\text{test})/p(\text{data}|\text{null}))$  for the combined CDF and D0 searches are shown in Fig. 12b–c for the hypothesis that an exotic particle is present with  $\mu_{\text{exotic}} = 1$ . Upper limits are calculated at 95% credibility on the production rate for an exotic Higgs boson in the absence of a SM signal to be 0.36 times the SM Higgs boson production rate for both of the exotic spin and parity hypotheses. Setting the production rate times branching fraction of the hypothetical exotic particle to the SM prediction for  $H \rightarrow b\bar{b}$ , the models with  $J_P = 0^-$  and  $J_P = 2^+$  are excluded with a significance of 5.0 s.d. and 4.9 s.d., respectively.

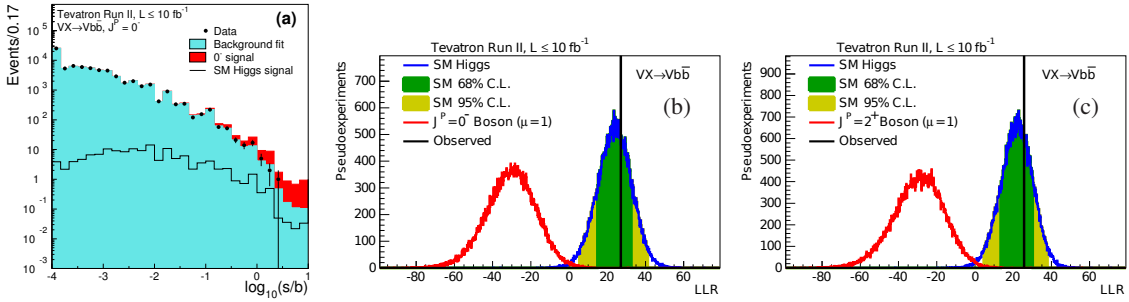


**Figure 12:** Distribution (a) of  $\log_{10}(s/b)$  for the combined CDF and D0 data computed from all channels contributing to the  $J_P = 0^-$  search. LLR distributions for assuming an exotic particle is present with  $\mu_{\text{exotic}} = 1$  and SM backgrounds for the models (b)  $J_P = 0^-$  and (c)  $J_P = 2^+$ .

## 6. Summary

The Tevatron legacy continues to expand with a rich, competitive and complementary physics program exploiting unique advantages afforded by collecting the world's highest energy  $p\bar{p}$  collision data, advantageous  $S/B$  ratios, triggering capabilities, and precise evaluations of detector performance. Recent results and those in progress include: precision EW measures, including fundamental parameters of the standard model ( $W$  mass,  $\sin^2\theta_W$ ),  $W/Z$  production and constraints for global fits for PDF models; world class top mass results, unique and complimentary measures in the top sector ( $A_{FB}$ , cross sections, decay properties, single top); an extensive b-physics program (CPV studies, hadron properties, new work in production and hadronization asymmetries); closing the gaps between earlier results and those from the LHC for moderately high mass new physics; limits on an exotic Higgs boson to fermions; and unique and complimentary work in QCD ( $V(V)+\text{jets}/\text{HF}$ , low- $x$  measurements, extensive studies of multiparton interactions.).

## References

- [1] V. M. Abazov *et al.*, Phys. Rev. Lett. **114**, 062001 (2015).
- [2] K. A. Olive *et al.* (Particle Data Group), Chin. Phys. C **38**, 090001 (2014); Y. Amhis *et al.* (Heavy Flavor Averaging Group Collaboration), arXiv:1207.1158, with web update at [http://www.slac.stanford.edu/xorg/hfag/osc/PDG\\_2014/](http://www.slac.stanford.edu/xorg/hfag/osc/PDG_2014/).
- [3] Y. Amhis *et al.* (Heavy Flavor Averaging Group Collaboration), arXiv:1412.7515, and online update at <http://www.slac.stanford.edu/xorg/hfag>.
- [4] T. Aaltonen *et al.* (CDF Collaboration) Phys. Rev. D **90**, 111103(R) (2014).
- [5] V. M. Abazov *et al.* (D0 Collaboration) Phys. Rev. D **90**, 111102(R) (2014).
- [6] M. Golden and B. Grinstein, Phys. Lett. B **222**, 501 (1989); A. Le Yaouanc, L. Oliver, and J.C. Raynal, Phys. Lett. B **292**, 353 (1992); F. Buccella, M. Lusignoli, G. Miele, A. Pugliese, and P. Santorelli, Phys. Rev. D **51**, 3478 (1995).
- [7] V. M. Abazov *et al.* (D0 Collaboration) Phys. Rev. Lett. **114**, 051803 (2015).
- [8] CDF note 11156, [http://www-cdf.fnal.gov/physics/new/top/2015/Afbbbbbar\\_lowm/publicAfb2.pdf](http://www-cdf.fnal.gov/physics/new/top/2015/Afbbbbbar_lowm/publicAfb2.pdf).
- [9] T. Aaltonen *et al.* (CDF Collaboration) Phys. Rev. D **92**, 032006 (2015).
- [10] V. M. Abazov *et al.* (D0 Collaboration) Phys. Rev. D **91**, 072008 (2015).
- [11] J. L. Rosner, Phys. Rev. D **90**, 014023 (2014).
- [12] D0 Conference Note 6464, <http://www-d0.fnal.gov/Run2Physics/WWW/results/prelim/B/B65/B65.pdf>.
- [13] W. K. Lai and A. K. Leibovich, arXiv:1410.2091 and private communications.
- [14] T. Aaltonen *et al.* (CDF Collaboration, D0 Collaboration) Phys. Rev. Lett. **115**, 152003 (2015).
- [15] N. Kidonakis, Phys. Rev. D **83**, 091503 (2011); S. Cortese and R. Petronzio, Phys. Lett. B **253**, 494 (1991).
- [16] N. Kidonakis, Phys. Rev. D **83**, 091503 (2011).
- [17] N. Kidonakis, Phys. Rev. D **81**, 054028 (2010).
- [18] T. M. P. Tait and C.-P. Yuan, Phys. Rev. D **63**, 014018 (2000)
- [19] V. M. Abazov *et al.* (D0 Collaboration), Phys. Rev. Lett. **99**, 191802 (2007)
- [20] J. Alwall *et al.*, Eur. Phys. J. C **49**, 791 (2007).
- [21] V. M. Abazov *et al.* (D0 Collaboration) Phys. Rev. D **91**, 112003 (2015).
- [22] V. M. Abazov *et al.* (D0 Collaboration), arXiv:1508.03322.
- [23] V. M. Abazov *et al.* (D0 Collaboration) Phys. Rev. D **91**, 032007 (2015); Erratum Phys. Rev. D **91**, 079901 (2015).
- [24] S. Frixione and B. R. Webber, J. High Energy Phys. **06** (2002) 029.
- [25] R. D. Ball *et al.*, Nucl. Phys. B **867**, 244 (2013).
- [26] V. M. Abazov *et al.* (D0 Collaboration) Phys. Rev. Lett. **115**, 041801 (2015).
- [27] V. M. Abazov *et al.* (D0 Collaboration), Phys. Rev. D **84**, 012007 (2011).

- [28] A. Banfi, S. Redford, M. Vesterinen, P. Waller, and T. R. Wyatt, *Eur. Phys. J. C* 71, 1600 (2011).
- [29] A. Banfi, M. Dasgupta, S. Marzani, and L. Tomlinson, *J. High Energy Phys.* 01 (2012) 044.
- [30] C. Balazs and C.-P. Yuan, *Phys. Rev. D* 56, 5558 (1997).
- [31] T. Aaltonen et al. (CDF Collaboration), CDF Note 11157, <http://www-cdf.fnal.gov/physics/ewk/2015/DibosonHF/>.
- [32] T. Aaltonen et al. (CDF Collaboration) *Phys. Rev. D* 91, 111101(R) (2015); Erratum *Phys. Rev. D* 92, 039901 (2015).
- [33] M.L. Mangano et al, *JHEP* 0307:001,2003, hep-ph/0206293.
- [34] E. Braaten, J. Lee, and S. Fleming, *Phys. Rev. D* 60, 091501 (1999); P. Artoisenet, F. Maltoni, and T. Stelzer, *J. High Energy Phys.* 02 (2008) 102.
- [35] T. Aaltonen et al. (CDF Collaboration) *Phys. Rev. D* 91, 052011 (2015).
- [36] V. M. Abazov et al. (D0 Collaboration) *Physics Letters B* 743 (2015).
- [37] V. M. Abazov et al. (D0 Collaboration) *Phys. Rev. D* 91, 052010 (2015).
- [38] T. Aaltonen et al. (CDF Collaboration) *Phys. Rev. Lett.* 115, 061801 (2015).
- [39] T. Aaltonen et al. (CDF Collaboration) CDF note 11102, <http://www-cdf.fnal.gov/physics/S15CDFResults.html>.
- [40] T. Aaltonen et al. (CDF Collaboration, D0 Collaboration) *Phys. Rev. Lett.* 114, 151802 (2015).
- [41] T. Aaltonen et al. (CDF and D0 Collaborations), *Phys. Rev. Lett.* 109, 071804 (2012); T. Aaltonen et al. (CDF and D0 Collaborations), *Phys. Rev. D* 88, 052014 (2013).
- [42] J. Ellis, D. S. Hwang, V. Sanz, and T. You, *J. High Energy Phys.* 11 (2012) 134.
- [43] T. Junk, *Nucl. Instrum. Methods A* 434, 435 (1999); A. L. Read, *J. Phys. G* 28, 2693 (2002); W. Fisher, FERMILAB-TM-2386-E (2006).